Demonstration of a six-dot quantum cellular automata system

Islamshah Amlani,[a] Alexei O. Orlov, Gregory L. Snider, Craig S. Lent, and Gary H. Bernstein
Department of Electrical Engineering, University of Notre Dame, Notre Dame, Indiana 46556

(Received 30 December 1997; accepted for publication 25 February 1998)

We report an experimental demonstration of a logic cell for quantum-dot cellular automata (QCA). This nanostructure-based computational paradigm allows logic function implementation without the use of transistors. The four-dot QCA cell is defined by a pair of series-connected double dots, and the coupling between the input and the output double dots is provided by lithographically defined capacitors. We demonstrate that, at low temperature, an electron switch in the input double dot induces an opposite electron switch in the output double dot, resulting in a polarization change of the QCA cell. Switching is verified from the electrometer signals, which are coupled to the output double dot. We perform theoretical simulations of the device characteristics and find excellent agreement with theory. © *1998 American Institute of Physics.* [S0003-6951(98)01417-X]

For many years, the microelectronics industry has enjoyed unfaltering growth by scaling down the size of electronic devices leading to higher speeds and denser circuit arrays. But, with the dimensions of conventional devices constantly contracting, and gate lengths shrinking toward the nanometer scale, it is becoming increasingly challenging to maintain the same pace of progress. As device feature sizes approach quantum limits, fundamental problems due to intrinsic quantum behavior are bound to be encountered. For continual growth, a paradigm that is more atuned to the properties of nanostructures holds the promise of faster speed, a lower power-delay product, and a higher level of integration.

A transistorless computation paradigm, known as quantum-dot cellular automata (QCA) architecture,[1–4] consists of nanometer-scale dots that are coupled through the Coulomb interaction. If their capacitances are sufficiently small, charge is quantized on the dots due to the Coulomb blockade of electron tunneling.[5] A basic QCA cell can be envisaged as a coupled-dot system with four dots located at the vertices of a square. Interdot tunneling may occur only in the vertical direction and interaction along the horizontal direction is governed by Coulombic fields. If the cell is charged with two excess electrons, they will occupy antipodal outer sites within the cell due to mutual electrostatic repulsion. These two polarization states of the cell can represent stable states of binary logic. All Boolean logic functions can be realized by an appropriate arrangement of these basic cells.

The operation of a QCA cell has been demonstrated experimentally in a four-dot system formed by two single dots and a double dot.[6] Here, we consider a more symmetric design, i.e., a pair of capacitively coupled, series-connected double dots, forming the QCA cell, and two single-dot electrometers. Figure 1 shows a schematic diagram of our six-dot QCA system. Dots D_1 and D_2 constitute the input double dot, and dots D_3 and D_4 form the output double dot. Capacitive coupling between the input and output double dots is provided by capacitors C_{1-3} and C_{2-4}. Each dot of the QCA cell is capacitively coupled to a gate electrode through capacitors $C_A - C_D$. In this letter, we will denote gates by these capacitors. Dots D_3 and D_4 are also capacitively coupled to the electrometer E_1 and E_2, respectively, in order to externally detect the polarization state of the output double dot.

The QCA cell of Fig. 1 is realized on an oxidized Si surface using standard Al tunnel junction technology pioneered by Dolan and Fulton.[7] Al islands and leads are patterned using electron-beam lithography with a subsequent shadow evaporation process and an intermediate *in situ* oxidation step. The area of the fabricated $Al/AlO_x/Al$ tunnel junctions is approximately $50\times 50\ nm^2$. The typical room-temperature tunnel resistance of the tunnel junction, determined from the $I-V$ measurements, is about 750 kΩ.

All measurements are carried out in a dilution refrigerator with a base temperature of 10 mK. Conductances of the double dots and electrometers are measured using standard ac lock-in techniques with an excitation voltage of 3 μV at 25–40 Hz. The experiment is performed in a magnetic field in order to quench the superconductivity of the Al metal at millikelvin temperatures. The capacitance of the tunnel junctions, extracted from the ''Coulomb gap'' of the electrometers, is approximately 240 aF. The other lithographic and parasitic capacitances are obtained from the Coulomb blockade oscillations of the double dots and electrometers. These capacitance parameters are used in our theoretical simulations of the device characteristics.

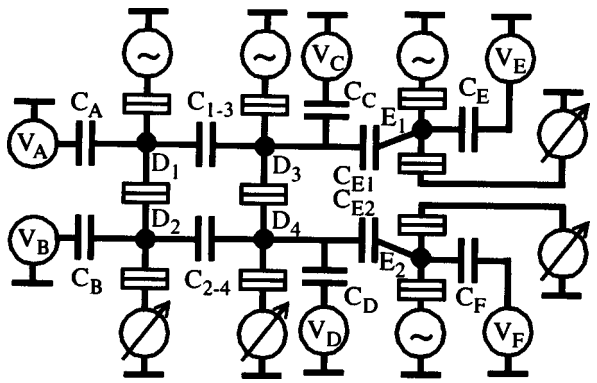

FIG. 1. Schematic diagram of the six-dot system.

[a]Electronic mail: Islamshah.amlani.l@nd.edu

 © 1998 American Institute of Physics
Downloaded 28 Mar 2007 to 129.74.250.197. Redistribution subject to AIP license or copyright, see http://apl.aip.org/apl/copyright.jsp

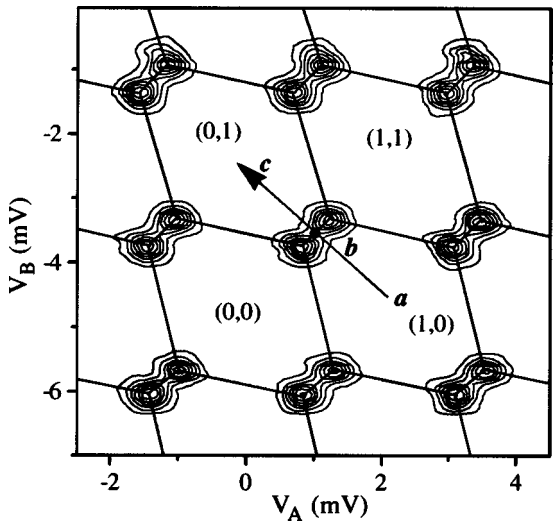

FIG. 2. Charging diagram of the input double dot as a function of the gate voltages V_A and V_B. Charge configurations (n_1,n_2), which represent the number of extra electrons on D_1 and D_2, respectively, are arbitrarily chosen.

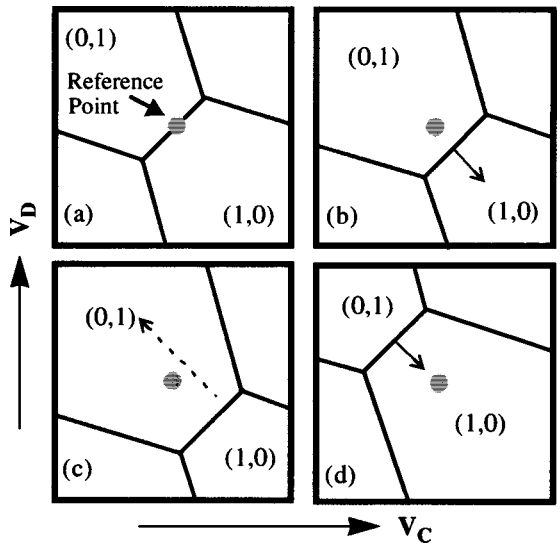

FIG. 3. Each plot corresponds to a particular setting of input diagonal voltage along the line $\overline{ac}$ as shown in the charging diagram of the input double-dot D_1–D_2 (Fig. 2). (a) Charge-exchange border of the output double dot (D_3–D_4) biased at the reference point. (b) Solid line with an arrow shows a gradual shift in the border position with respect to the reference point as the bias on D_1–D_2 varies from point a to b. (c) Dotted line with an arrow shows an abrupt reset in the border position coinciding with the input diagonal voltage crossing point b. (d) Border gradually shifts towards the reference point (shown by the solid line with an arrow) as the bias on D_1–D_2 varies from point b to c.

At the heart of the QCA operation is the double-dot charging diagram, which plays a vital role in determining the voltages that must be applied to the dots for a given QCA polarization. Figure 2 shows a contour plot of the conductance through the input double dot as a function of the gate voltages V_A and V_B. This plot is obtained by scanning gate C_A for an incremental setting of voltages on gate C_B. The conductance of a double dot with a nonzero interdot capacitance forms a honeycomb pattern,[8] delineated by solid lines that connect each triple point. In each cell, demarcated by hexagonal borders, a given charge configuration of the double dot (n_1,n_2) is the ground state with n_1 and n_2 representing the number of extra electrons on dots D_1 and D_2, respectively. As the honeycomb boundaries are crossed along the horizontal or the vertical direction, by scanning either gate C_A or C_B, electrons are sequentially added to that dot adjacent to the gate, while the population of the other dot remains constant. An electron exchange between D_1 and D_2 takes place along the charge-exchange direction, shown by the line $\overline{ac}$, where an electron moves from D_1 to D_2 leaving the total number of electrons on the two dots unaltered. QCA operation is executed by applying bias to gates C_A and C_B along this charge-exchange direction.

A polarization change of the QCA cell requires an electron exchange between dots within each double dot. This can be best visualized by examining the honeycomb patterns of the input and output double dots during the charge exchange. When a ''diagonal'' voltage is applied to the input gates (shown by direction $\overline{ac}$ in Fig. 2), the double dot is polarized. This, in turn, produces an electrostatic force on the coupling capacitors C_{1-3} and C_{2-4}, resulting in an opposite polarization switch of the output double dot. The polarization change of the output double dot is reflected in the displacement of its honeycomb pattern with respect to a fixed reference point.

Figure 3 illustrates how the honeycomb pattern of the output double dot (D_3–D_4) shifts in response to the electrostatic potential change on the input double dot (D_1–D_2). As the gate electrodes C_A and C_B are scanned in the charge-exchange direction $\overline{ac}$ (Fig. 2), the potential on D_2 linearly increases with the rising voltage V_B and the potential on D_1 decreases with the decreasing voltage V_A, until an abrupt potential reset in the opposite direction when an electron is transferred from D_1 to D_2. Since the potentials on D_1/D_2 act as extra gate voltages for D_3/D_4, the honeycomb pattern of the output double dot shifts as an electron switches from D_1 to D_2. This process is sequentially depicted for D_3–D_4 in Fig. 3 with each plot corresponding to a certain setting of diagonal voltage on D_1–D_2 (Fig. 2). Figure 3(a) shows the position of the reference point, which is biased at the honeycomb border between the (0,1) and (1,0) states. As the diagonal voltage on gates C_A and C_B is varied from point a to c of Fig. 2, the honeycomb pattern for D_3–D_4 first moves away from the reference point [Fig. 3(b)], resets abruptly as the diagonal bias on D_1–D_2 crosses point b [shown by the dotted line in Fig. 3(c)], and then moves back towards the reference point [Fig. 3(d)]. If the shift in the D_3–D_4 honeycomb border, caused by an electron switching in D_1–D_2, is sufficient to move it from one side of the reference point to the other, then an electron switches from D_4 to D_3.

In order to verify experimentally that an electron switching in D_1–D_2 brings about an opposite electron switch in D_3–D_4, we measure the conductances of electrometers E_1 and E_2, simultaneously, as we vary the input diagonal voltage from point a to c. Electrometers are sensitive to small charge excursions on their capacitively coupled dots[9] and can externally detect when an electron switches in D_3–D_4. To ensure an identical response from each electrometer, both are biased, using C_E and C_F, on a positive slope of their conductance peak prior to the experiment. The reference point for the output double dot is also biased near the charge-exchange border using gates C_C and C_D. Figure 4(a) shows

Downloaded 28 Mar 2007 to 129.74.250.197. Redistribution subject to AIP license or copyright, see http://apl.aip.org/apl/copyright.jsp

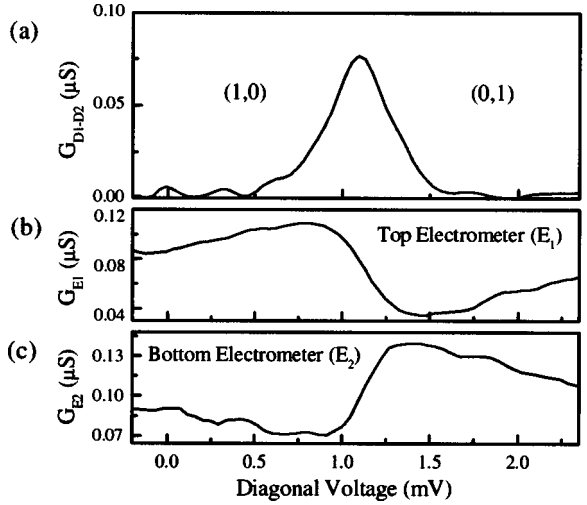

FIG. 4. (a) Conductance through the input double dot as a function of the diagonal voltage. The peak indicates the switch of an electron from D_1 to D_2. (b) Conductance through E_1 indicating the addition of an electron to D_3. (c) Conductance through E_2 indicating the removal of an electron from D_4.

the conductance through D_1-D_2 as a function of the diagonal voltage. We see that the conductance peaks at the saddle point delineating a border between the two charge states (1,0) and (0,1). As an electron switches from D_1 to D_2, it induces an opposite electron switch in D_3-D_4, i.e., (0,1), to (1,0), which is reflected in the conductances of the electrometers [Figs. 4(b) and 4(c)]. The conductance of E_1 increases linearly with an abrupt shift when an electron enters D_3. Likewise, the conductance of E_2 decreases with an abrupt shift when an electron vacates D_4. This denotes a polarization change of the QCA cell.

We compare the measured potential change on dot D_3 during QCA switching with theoretical results. Figure 5(a) shows the experimental and theoretical plots of the potential on dot D_3 as a function of the input diagonal voltage. The experimental plot for the potential on D_3 is computed from the conductance of E_1. In the simulation, we use all interdot, dot-to-gate, and dot-to-ground capacitances as measured prior to the experiment. The theoretical results are obtained by minimizing the classical electrostatic energy for all six dots and the voltage leads. Minimum energy-charge configurations are calculated for each setting of the input diagonal voltage, given the condition that the charge on each dot of the QCA cell be an integer multiple of e. The effect of nonzero temperature on the potential and the charge is simulated by thermodynamic averaging over all nearby charge configurations. From Fig. 5(a), we can see that the agreement between experiment and theory is excellent with only the substrate background charge and temperature as fitting parameters. Background charge adds only an offset in the position of the peak and has no influence on the magnitude or the period of the dot potential. The best fit to experiment is obtained for 75 mK, which is in close agreement with the actual device temperature, as verified from the peak-shape analysis for different temperatures.[10] The discrepancy in the base temperature of the refrigerator and the actual device temperature is most likely due to heating of the electron subsystems and insufficient filtering of the leads.

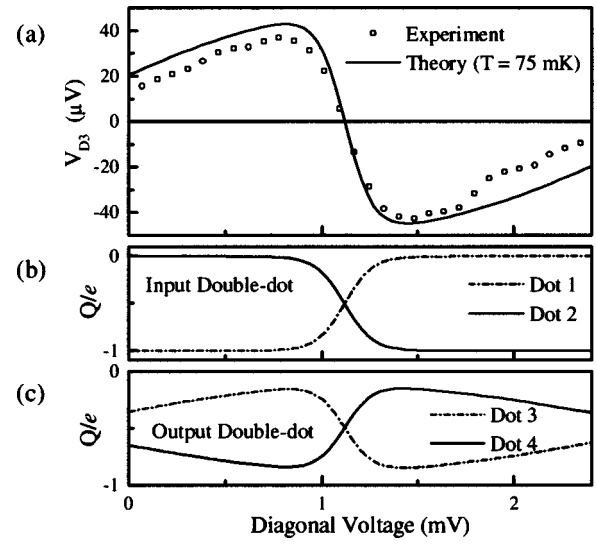

FIG. 5. (a) Experimental and theoretical curves showing the potential change on dot D_3 as a function of the input diagonal voltage. The solid line represents the simulation result at 75 mK, and the dotted line shows the experimental values calculated from the conductance of E_1. (b) Theoretical calculations of the charges on dots D_1 and D_2, and (c) dots D_3 and D_4 during QCA polarization change.

To confirm that the potential switch on D_3 [Fig. 5(a)] indicates a polarization change of the QCA cell, we also compute excess charge on each dot as a function of the input diagonal voltage. Figure 5(b) shows a 100% polarization change in the input double dot as an electron is transferred from D_1 to D_2. Figure 5(c) shows an opposite polarization change in the output double dot as an electron switches from D_4 to D_3. The results show a 70% polarization change in the output double dot, which can be further enhanced by increasing the coupling capacitances C_{1-3} and C_{2-4}.

In summary, we have presented measurements of a four-dot QCA logic cell capacitively coupled to two single-dot electrometers. We have exploited Coulomb blockade effects to demonstrate that if the cell is charged with two extra electrons, then the polarization of the cell can be changed by applying bias to the input gates. Switching in the cell is verified by the electrometer signals, which show an opposite polarization change in the output double dot under the influence of an electron switching in the input double dot. Results obtained from the theoretical simulations of the QCA switching strongly support the experimental data.

This research was supported in part by DARPA, ONR (Grant No. N0014-95-1-1166) and NSF. The authors wish to thank W. Porod and J. Merz for helpful discussions.

[1] C. S. Lent, P. D. Tougaw, and W. Porod, Appl. Phys. Lett. **62**, 714 (1993).
[2] P. D. Tougaw, C. S. Lent, and W. Porod, J. Appl. Phys. **74**, 3558 (1993).
[3] C. S. Lent, P. D. Tougaw, W. Porod, and G. H. Bernstein, Nanotechnology **4**, 49 (1993).
[4] C. S. Lent and P. D. Tougaw, J. Appl. Phys. **75**, 4077 (1994).
[5] *Single Charge Tunneling*, edited by H. Grabert and M. H. Devoret (Plenum, New York, 1992).
[6] A. O. Orlov, I. Amlani, G. H. Bernstein, C. S. Lent, and G. L. Snider, Science **277**, 928 (1997).
[7] T. A. Fulton and G. H. Dolan, Phys. Rev. Lett. **58**, 109 (1987).
[8] H. Pothier, P. Lafarge, C. Urbina, D. Esteve, and M. H. Devoret, Europhys. Lett. **17**, 249 (1992).
[9] P. Lafarge, H. Pothier, E. R. Williams, D. Esteve, C. Urbina, and M. H. Devoret, Z. Phys. B **85**, 327 (1991).
[10] U. Meirav, P. L. McEuen, M. A. Kastner, E. B. Foxman, A. Kumar, and S. J. Wind, Z. Phys. B **85**, 357 (1991).

Downloaded 28 Mar 2007 to 129.74.250.197. Redistribution subject to AIP license or copyright, see http://apl.aip.org/apl/copyright.jsp